

Defect states in red-emitting $\text{In}_x\text{Al}_{1-x}\text{As}$ quantum dots

R. Leon and J. Ibáñez

Jet Propulsion Laboratory, California Institute of Technology, 4800 Oak Grove Drive, Pasadena, California 91109

S. Marcinkevičius and J. Siegert

Department of Microelectronics and Information Technology, Royal Institute of Technology, Electrum 229, 164 40 Kista, Sweden

T. Paskova and B. Monemar

Department of Physics and Measurement Technology, Linköping University, S-581 83, Linköping, Sweden

S. Chaparro, C. Navarro, S. R. Johnson, and Y.-H. Zhang

Center for Solid State Electronics Research and Department of Electrical Engineering, Arizona State University, Tempe, Arizona 85287

(Received 13 May 2002; published 30 August 2002)

Optical and transport measurements carried out in *pn* diodes and Schottky barriers containing multilayers of InAlAs quantum dots embedded in AlGaAs barriers show that while red emission from quantum dot (QD) states is obtained at ~ 1.8 eV, defect states dominate the optical properties and transport in these quantum dots. These defects provide nonradiative recombination paths, which shortens the carrier lifetimes in QD's to tens of picoseconds (from ~ 1 ns) and produce deep level transient spectroscopy (DLTS) peaks in both *p* and *n* type structures. DLTS experiments performed with short filling pulses and bias dependent measurements on InAlAs QD's on *n*-AlGaAs barriers showed that one of the peaks can be attributed to either QD/barrier interfacial defects or QD electron levels, while other peaks are attributed to defect states in both *p* and *n* type structures.

DOI: 10.1103/PhysRevB.66.085331

PACS number(s): 78.66.Fd, 73.40.Gk

INTRODUCTION

The role that defects play on quantum dot properties is interesting from several perspectives. Radiation induced defects appear to have much lesser effects in diminishing radiative emission from quantum dot (QD) luminescent structures and QD laser diodes^{1,2} than in quantum well (QW) or bulk structures. Higher intensities have even been observed after proton and ion induced displacement damage in QD structures. These can be explained by defect assisted carrier relaxation, and by defect assisted tunneling in cases with potential barrier surrounding QD's.³

The effects of dislocation defects on QD properties are also of interest due to several promising technological applications. The growth of multistacked planes containing quantum dots is used to increase gain in lasers. If the cumulative strain from several dot layers exceeds the critical thickness for plastic relaxation^{4,5} then a misfit dislocation can be formed at the buffer layer/quantum dot interface in multistacked dot layers. Such misfit dislocations might form spontaneously in some structures, however, strong radiative emission from QD states is still present in these cases. Another application where dislocation defects are relevant involves the attempts to obtain positional order in QD's. In this type of growth, QD's are grown on strain relaxed GeSi or InGaAs epitaxial films, and they have been shown to have rectangular alignment, presumably from the dislocation shear steps at the surface.^{6,7} Another interesting application where dislocations can play an important role is in the growth on InAs QD's on GaAs/Si.^{8,9} QD device applications in such structures have the potential of enabling Si optoelectronic devices, and of integrating logical and optical functions in system-on-a-chip applications.

Impurities introduced unintentionally during growth can have an important role in the properties of QD containing structures, and are believed to be responsible for the short luminescence lifetimes observed in some InAlAs/AlGaAs QD's.¹⁰ It is also well known, that interfacial defects as those formed during *ex-situ* processing in etched quantum dots have a strong role on their optical properties as well.^{11,12}

The use of deep level transient spectroscopy (DLTS) in the characterization of deep levels in semiconductors is well established. DLTS has also been used to attempt determination of eigen-states from electron and hole levels in InAs quantum dots.¹³⁻¹⁵ The literature on this topic has given some conflicting information, and the interpretation of results is not always straightforward. To complicate matters, it is quite possible to have defect states in samples that also contain QD's; therefore, differentiation of DLTS signals originating from defects or from electron or hole energy levels can be ambiguous.

Here we use optical and electrical measurements to study the role of impurities and unintentional defects introduced during growth in InAlAs QD's in both *p* and *n* AlGaAs barriers. The results shown here demonstrate that unlike radiation induced damage, or dislocation effects from the barrier layer under the dots, these defects have a prominent role in the optical and transport properties of these QD structures. DLTS experiments show different behaviors from peaks in *p* and *n* type samples. Measurements carried out at different reverse biases and experiments performed varying the filling pulse times allowed determination of trap activation energies, trap densities, and capture cross sections. In this work we show that these defects affect the optical properties of these quantum dots due to their localization either within the dots or at their interfaces. This is in contrast to what is ob-

served from radiation induced defects,¹⁻³ which are randomly distributed, and the majority are formed in the barrier material, and spatially separated from the QD region, where they do not contribute significantly to nonradiative recombination due to wave function confinement in the QD's.

EXPERIMENTAL DETAILS

Two QD structures were grown by molecular beam epitaxy. The structures consist of 50-nm layers of *n*-type (*p*-type) $\text{Al}_{0.33}\text{Ga}_{0.67}\text{As}$ terminated with $\text{In}_{0.45}\text{Al}_{0.55}\text{As}$ QD's (using five monolayers coverage), repeated eight times on top of a 300-nm-thick n^+ doped ($n^+ = 1 \times 10^{18} \text{ cm}^{-3}$) AlGaAs layer and a 100-nm-thick n^+ doped ($n^+ = 1 \times 10^{18} \text{ cm}^{-3}$) GaAs buffer layer. Si and Be were used for *n* and *p* dopants with nominal doping $n = p = 10^{17} \text{ cm}^{-3}$. A final $\text{Al}_{0.3}\text{Ga}_{0.7}\text{As}$ layer with the same doping level was deposited and capped with a thin GaAs layer to prevent oxidation of the AlGaAs. A top Schottky diode and back Ohmic contacts were formed for the *n*-type sample and back and top Ohmic contacts were formed on the *p*-type sample. Two additional samples with doped AlGaAs barriers and no InAlAs quantum dots were also grown as control structures, and processed in a similar manner. Analysis of island sizes and densities using atomic force microscopy in air gives average diameters of 20 nm (5 nm heights) and concentrations of $1 \times 10^9 \text{ cm}^{-2}$ for uncapped InAlAs QD's grown under the same conditions. Capacitance voltage measurements were carried out at variable temperature (20 to 300 K). Deep level transient spectroscopy was carried out from 20 to 315 K at delay time τ in the (0.02–100) ms range and at a rate window of $4.3 \times \tau$. Low-temperature cathodoluminescence (CL) imaging and spectroscopy were carried out using a scanning electron microscope equipped with a cryogenic stage and a monochromator attachment for CL spectroscopy. CL was performed imaging the structures in cross section, at temperatures between 4.5 and 10 K using an accelerating voltage of 5 KeV. Carrier dynamics were studied by time-resolved photoluminescence (TRPL) at 80 K after excitation by frequency-doubled femtosecond laser pulses at 400 nm from a Ti:sapphire laser. The PL was detected using a synchroscan streak camera, combined with a 0.25 m spectrometer (temporal resolution 3 ps).

RESULTS

Cathodoluminescence

A typically broad emission in the visible (red) region is apparent in the CL spectra displayed in Fig. 1. The peaks found are at 660–675 nm (1.843 and 1.857 eV with inhomogeneous broadening of 37 and 26 meV, respectively). Monochromatic CL imaging (not shown here) using the peak wavelengths in both *n* and *p* samples (imaged in cross section) did show that the signal originated from the 40 nm region containing the multilayered InAlAs QD's, hence we attribute these CL peaks to radiative recombination from QD states. The absence of any emission from AlGaAs is apparent as a dark region from the layer under the QD structures in CL imaging mode, even though AlGaAs related peaks ~ 2 eV have been observed in previous studies of similarly

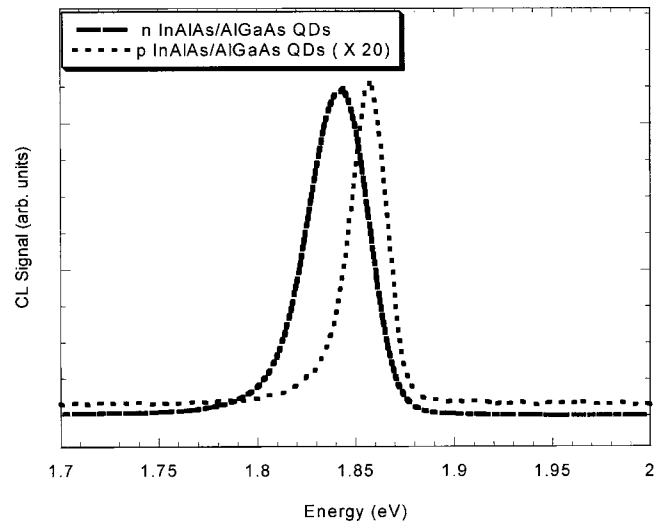


FIG. 1. Cathodoluminescence spectra from the eight-layer QD regions in *n*- and *p*-InAlAs/AlGaAs structures.

grown InAlAs/AlGaAs QD's.^{16,17} The control structures showed no CL from the active region. Emission from the GaAs at 831 nm was seen in all structures, with a stronger intensity from the GaAs buffer layer below the AlGaAs barrier.

Time resolved photoluminescence

Figure 2 shows PL transients from these QD structures. Some weak PL emission from the control samples (containing only the *p* and *n* doped AlGaAs barrier films) can be detected by TRPL, although these were not observable with the CL setup that was used at temperatures of 4.5 K. Figure 2 shows results from *p*- and *n*-InAlAs quantum dots as well

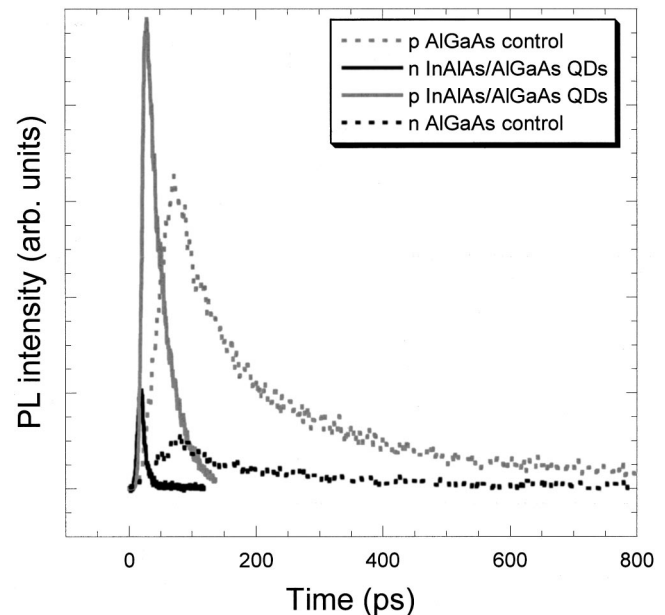


FIG. 2. Time resolved photoluminescence from *p*- and *n*-InAlAs/AlGaAs quantum dots. TRPL is also shown from the *p* and *n* control samples.

as from the control sample barrier emission. These measurements indicate PL decay times of 6 and 29 ps for the n - and p -type $\text{InAlAs}/\text{AlGaAs}$ QD's, respectively. These are significantly shorter than the decay from the weaker AlGaAs emission in the control structures, which were 88 and 85 ps for the n and p structures, respectively. In InAs and InGaAs QD structures, where carrier dynamics are not dominated by non-radiative recombination, PL decay times measured at similar temperatures have been reported in the range (1–5) ns.^{18,19} Decay times from $\text{InAlAs}/\text{AlGaAs}$ QD's grown by MOCVD and MBE have been reported in the range (300–500) ps.^{18,20}

Electrical measurements (C - V and DLTS)

In order to further characterize the origin of the nonradiative recombination centers responsible for the short QD PL decay times observed in both n and p $\text{InAlAs}/\text{AlGaAs}$ quantum dot structures, electrical measurements were performed using DLTS and C - V analysis. Capacitance voltage was performed at various temperatures in order to determine the electron and hole concentration (majority carriers) in these samples. These measurements allowed quantitative determination of electron and hole trap densities and estimations of the space charge region at the various values of reverse bias used in DLTS. From C - V analysis it was found that the carrier concentration drops sharply below 180 K for the n type samples, and below 150 K for the p type structures (from an initial shallow acceptor or donor concentration of $2 \times 10^{17} \text{ cm}^{-3}$ at room temperature). This rapid drop is due to carrier freeze-out and it accounts for the variation in DLTS peak intensity found at different time windows in the DLTS measurements.

DLTS in $\text{InAlAs}/p\text{-AlGaAs}$ quantum dot structures

DLTS of the p structures was performed for various values of reverse bias, filling pulse duration and delay time windows.²¹ Figure 3 shows a typical spectrum taken at delay times of 0.2 ms, and reverse bias of -1 V. Spectra were collected from values of time windows between 0.02 and 100 ms, and at reverse bias voltages from -0.5 to -1.5 V. Activation energies were evaluated from all spectra, a typical Arrhenius plot is shown in the inset of Fig. 3. The values for the activation energy (E_a) did not vary significantly with reverse bias (E_a ranged from 0.35 to 0.39 eV) averaging 0.37 eV. The peak shape did not change with filling pulse duration, but its intensity changed. This was used to measure the value of the main trap capture cross section directly. As is expected and common in most DLTS spectra, the peak shape did not change with applied bias, and the peak intensity increased monotonically with increased bias. Trap concentrations (N_t) were evaluated for this peak from the relation

$$N_t = (2\Delta C/C)N_{d,a}.$$

N_t was found to be $\sim 6 \times 10^{16} \text{ cm}^{-3}$.

Figure 3 also shows a lower intensity peak at lower temperature (130 K). This peak was only present when DLTS spectra were acquired using longer delay times, and it did not change intensity in proportion to applied bias. Convolution

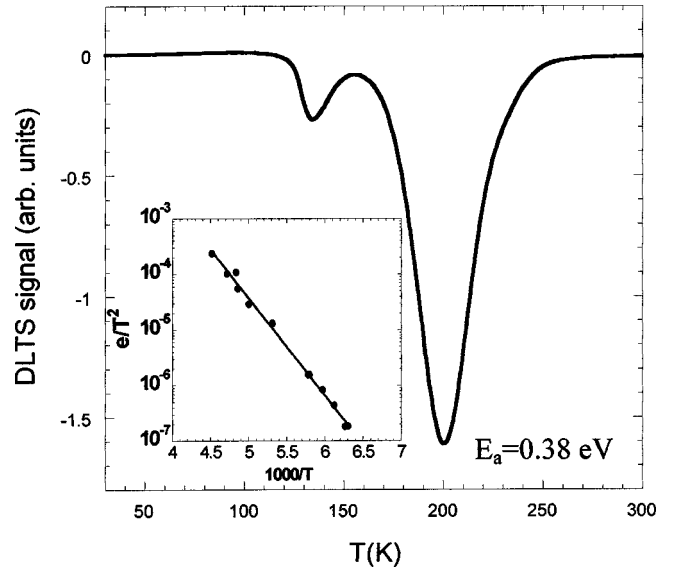


FIG. 3. DLTS spectra for from p - $\text{InAlAs}/\text{AlGaAs}$ QD structures, for delay time of 0.2 ms (emission rate of 0.86 ms), at -1 V applied bias, and $1 \mu\text{s}$ pulse duration. The inset shows Arrhenius plot for 12 values of delay times from the main peak.

effects from the main (more intense) peak did not allow determination of activation energy from this peak.

DLTS measurements were also performed on the control p - AlGaAs samples. No signal was observed even at much higher gains than used in the measurements on the structures containing the InAlAs quantum dots.

DLTS in $\text{InAlAs}/n\text{-AlGaAs}$ quantum dot structures

Similar DLTS experiments as described in the previous section were performed on n type InAlAs quantum dot structures. In these experiments, several “anomalies” were observed. At long values of filling pulse time (from 1 to 100 ms) the DLTS spectra shows a complex structures, with at least three convoluted peaks. Variation of time windows showed a change in peak shape, indicating different values for activation energies from the different peaks. The complex nature of the spectra did not allow determination of single activation energies for spectra acquired using these long filling pulse times.

DLTS measurements performed on the control n - AlGaAs structures did not show any of the peaks found in the $\text{InAlAs}/\text{AlGaAs}$ structures. A different peak was found at higher temperatures, however, its intensity was at least an order of magnitude lower than the ones reported for the $\text{InAlAs}/\text{AlGaAs}$ structures.

Further experiments performed using shorter “filling” pulses were carried out in these structures. The aim was to eliminate the signal from traps with small capture cross sections by using short filling pulses, and possibly analyze any remaining peaks that might have larger capture cross sections. Surprisingly, when the filling pulses were reduced (1 to 10 μs), a dramatic change in the spectra was observed. The complex peak structure disappeared, and instead, a simple peak (but broader than most defect related peak) remained.

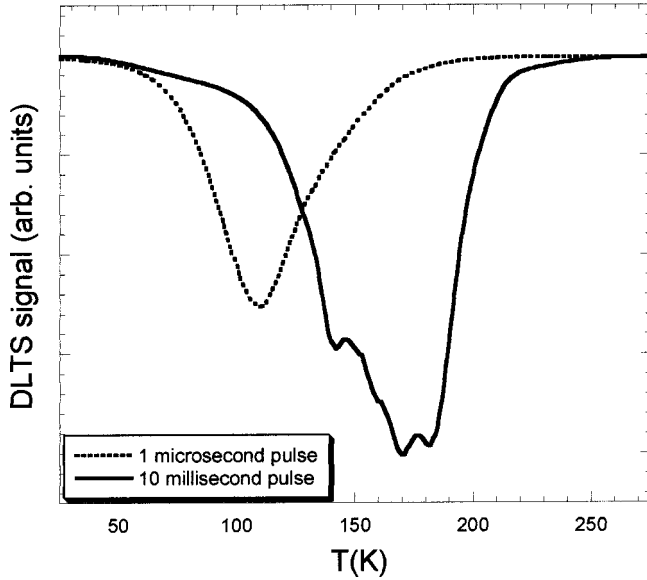


FIG. 4. DLTS spectra from *n*-InAlAs/AlGaAs QD structures obtained for very short filling pulses (1 μ s) at various applied reverse bias voltages for a delay time of 0.5 ms.

This peak appeared at lower temperature, and it was much more intense than what was observed as a very weak shoulder in the experiments performed with long filling pulses. DLTS spectra were then taken using different delay times and different applied reverse biases. The experiments at different reverse biases showed several unusual features. The peak shape changed with reverse bias, becoming narrower at higher values of applied bias. These changes are shown for several bias values in Fig. 4. The intensity of the signal was compared for the various biases by integrating the peaks in order to account for the changes in the peak shapes. The signal intensities do increase with applied bias, but they show at least three well-defined plateaus. Activation energies obtained from the different Arrhenius plots were evaluated. A general increase in activation energy can be seen with increased applied biases ranging from 0.5 to 3.25 V. The increase is not monotonic but the general trend is towards higher activation energies with larger applied biases. Measurement of trap concentrations from this peak was also evaluated from the signal intensity and measured carrier concentration and found to be $\sim 3 \times 10^{14} \text{ cm}^{-3}$ at -1 V applied reverse bias.

Experimental measurements of trap carrier cross sections

Capture cross sections can be measured for traps by varying the “fill” pulse duration and recording the change in signal intensity for a given peak. As reported in earlier studies,^{22,23} capture cross sections can be measured directly in DLTS using the relation

$$\Delta C(t_p)/\Delta C(t_p \rightarrow \infty) = 1 - e^{(-\sigma e \langle v_{th} \rangle t_p)},$$

where σ is the capture cross section, e the carrier concentration, $\langle v_{th} \rangle$ is the thermal velocity, and t_p is the filling pulse duration.

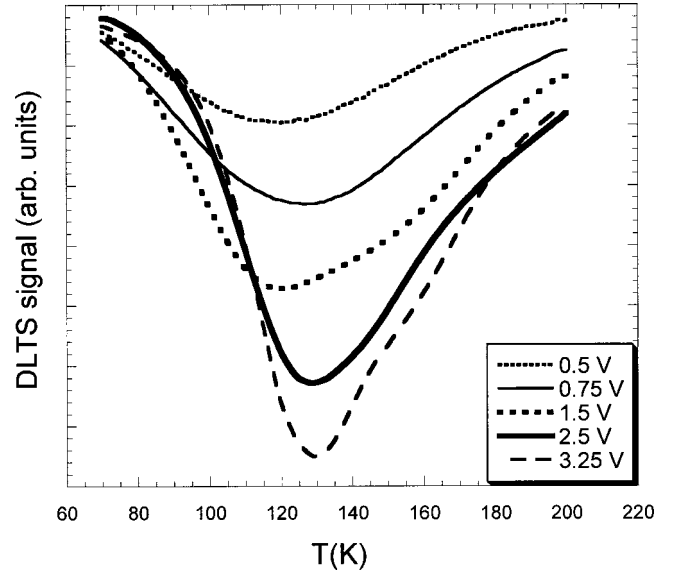


FIG. 5. DLTS signal intensity as a function of filling pulse for the main peak in the *p*-type InAlAs/AlGaAs quantum dots and for the peak obtained at short filling pulse times in the *n*-InAlAs/AlGaAs QD structures. Measurements were done at the temperatures for maximum peak intensity (120 K in *n*-InAlAs/AlGaAs and 186 K for *p*-InAlAs/AlGaAs) and 0.5 ms delay times in both cases.

Capture cross section measurements were performed for the main peak seen in the *p*-QD samples and for the main peak studied in the *n*-QD samples (the remaining peak after 1 μ s fill pulse). These are plotted for both peaks in Fig. 5. For the *n*-type structures, the peak intensity reaches a maximum and then decreases with long filling pulses, which is consistent with the unusual low temperature peak increase shown in Fig. 6. The maximum peak intensity in this case occurs for filling pulse time of 30 μ s.

Better fits were obtained for the shorter times. In the *n*-type samples, this can be explained with the unusual behavior of the lower temperature peak for longer fill times, and also by peak distortion due to the appearance of the multipeak structure due to the increased importance of defects with smaller capture cross sections at longer fill times. Fits to the experimental data shown in Fig. 5 show larger capture cross sections from the traps found in the *n*-type samples with small filling pulses, as compared to the traps found in the *p*-type samples. Values for the capture cross sections were $\sim 1 \times 10^{-17} \text{ cm}^2$ in the *n*-type samples vs $1 \times 10^{-19} \text{ cm}^2$ in the *p*-type samples.

DISCUSSION

These results, which combine optical and transport measurements, clearly show that a strong interaction exists between defect centers, and quantum dot states in both types of structures (with *n*- and *p*-doped barriers). The very short PL decay times originating from the QD emission was the first indication of the strong role of defect levels on the properties of these QD's, since PL decay times in the QD's are much shorter than values obtained in earlier measurements of PL lifetimes in InAs, InGaAs, and InAlAs quantum dots. Since

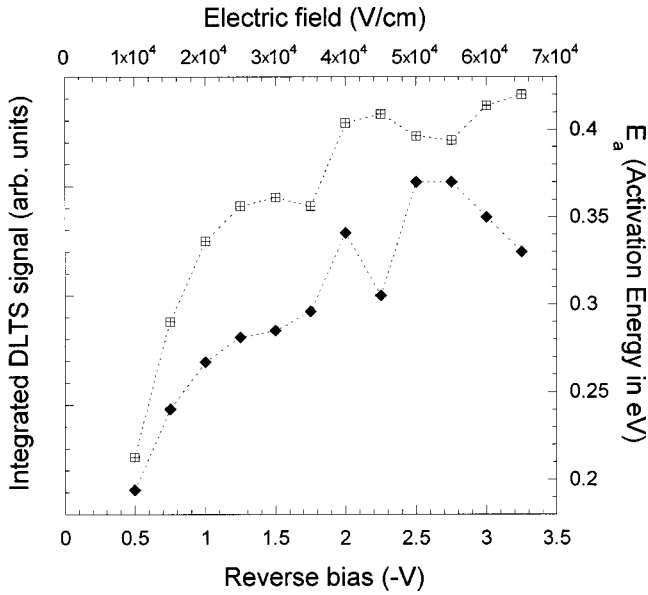


FIG. 6. DLTS spectra (at -4 V reverse bias and 100 ms delay time) from n -InAlAs/AlGaAs QD structures. The peaks are shown at their corresponding relative intensities, for very short filling pulse times and long filling pulse times.

the PL decay times in the QD's are also much shorter than in the control samples (without the quantum dots), it is probable that defect levels responsible for the short carrier lifetimes in the dots are either within the dots or at the dot/barrier interface. PL decay times in doped samples gives minority carrier lifetimes.²⁴ Estimation of trap densities in p - and n -type structures give $6 \times 10^{16}/\text{cm}^3$ for the InAlAs/ p -AlGaAs samples vs $3 \times 10^{14}/\text{cm}^3$ for the InAlAs/ n -AlGaAs samples. However, the trapping rates ($1/\tau$) are proportional to trap concentrations multiplied by capture cross sections (and the thermal velocity). Here we have more traps in the p samples, but also a much smaller cross section. The product of the concentration and cross section is only twice as large in the p structure than in the n structures. If we multiply further by the thermal velocity, the rate in the n sample is larger than in the p sample, which can explain the shorter lifetime in the n than in the p structures.

One of the difficulties using DLTS to characterize quantum dots in an environment that also contains traps due to defect related levels, is the ambiguity in differentiating which signal originates from defects and what is due to the QD electron or hole levels, since both of them can produce DLTS signals. We believe the main peak found in the DLTS spectra from the p -type structure, with $E_a \sim 0.37$ eV, originates from defect levels, rather than QD levels. The two main arguments for attribution of this hole trap to a defect related trap, rather than from hole levels in quantum dots, are the trap activation energy (E_a) and the trap level concentration (N_t). If these originated from QD hole levels, 0.37 eV would be the energy spacing from the barrier valence band to the hole level; and this is much too large to be explained by a hole level. Also, the hole and electron level concentrations would have to scale with the known quantum dot concentration in the small volume probed by our measurements

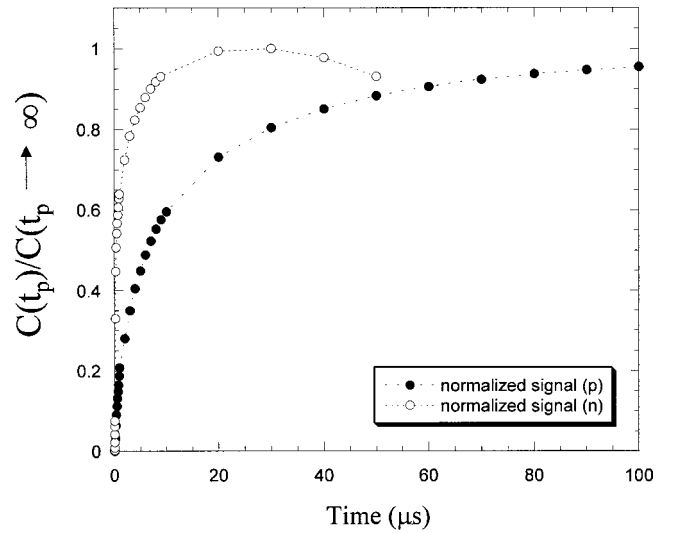


FIG. 7. Integrated DLTS signal (hollow symbols) as a function of applied reverse bias from n -InAlAs/AlGaAs QD structures. Also plotted are activation energies extracted from Arrhenius plots of DLTS spectra taken at various values of applied reverse bias.

$\sim 2-3 \times 10^{14}/\text{cm}^3$, which is too low to account for $N_t \sim 6 \times 10^{16}/\text{cm}^3$.

Unlike the well studied and controversial D - X centers in n -type AlGaAs, there have been few reports of any important defects levels in p -AlGaAs. The absence of any DLTS peaks from the control p -AlGaAs structures used here agrees with this observation. We believe that this 0.37 eV hole trap is related to the presence of InAlAs, however, it does not behave similar to other known interface defects, in the sense that the signal strength increases monotonically with reverse bias. This is in contrast to the sharply increasing DLTS signal shown in Fig. 7 for the peak found at short filling pulses in the n -InAlAs samples, and to the sharply increasing signal attributed to interfacial defects in other reports that include AlGaAs based superlattices.²⁵ Hole traps in AlGaAs devices have been reported in n -type AlGaAs/InGaAs PHEMT's which were attributed to surface states at ungated AlGaAs regions, but their reported activation energies were much higher than the $E_a = 0.37$ eV measured in this work.²⁶

DLTS analysis in the InAlAs/ n -AlGaAs structures presents an even more complex picture. The multiple peak structure found at longer filling pulse times is similar to what other studies have found for DX -like centers in GaAs/AlGaAs superlattices.^{27,28}

The increase in intensity with diminishing filling pulse times observed from the low-temperature peak is very unusual, and to our knowledge, has never been reported. The observation of plateaus in the integrated DLTS signal intensity rule out a uniform defect distribution, and are consistent with the signal originating from the different QD layers. From the measured free electron concentrations, calculations of depletion widths for Schottky barriers and pn junction geometries were made at different reverse bias levels. These give depletion widths of 420, 340, 265, and 152 nm at biases of -3 , -2 , -1 , and 0 V. These agree quite well with the interpretation of the signals originating from 2, 3, and 5 lay-

ers of QD's at biases of -1 , -2 , and -3 V (there are three quantum dot layers within the space charge region at zero bias). Here, unlike in the case shown earlier for the InAlAs/ p -AlGaAs samples, the trap density is very close to the volumetric estimates of QD in the region probed by the electrical measurements ($3 \times 10^{14} \text{ cm}^{-3}$ vs $\sim 2-3 \times 10^{10} \text{ cm}^{-3}$), therefore, we cannot rule out the possibility that this trap level originates from electron levels in the InAlAs quantum dots. These observations, the peak behavior with applied bias and the defect trap concentration, lead us to conclude that this peak originates either from an interfacial defect, most likely from the InAlAs/AlGaAs interface; or from electron levels in the InAlAs QD's. As was reported in earlier studies,^{11,12,29} interfacial defects have been known to give strong DLTS signals and are also known to hamper radiative recombination from QD states. Interfacial defects have been observed^{25,26} to have a rapid increase in signal intensity with applied bias as the bias sweeps over the interfacial region. An unambiguous identification of the origin of this broad low-temperature peak that is seen mainly for short filling pulses in InAlAs/ n -AlGaAs QD's can only be made if the defect concentration can be reduced to a much lower density than the QD volumetric density, which will require additional growth optimization in future work.

The most unusual features seen in Figs. 6 and 7 are the increased intensity of the low-energy peak with shorter filling pulses, and the shift in activation energies with increased reverse bias. This field dependence is different from what would be expected from the Poole Frenkel effect,³⁰ since the thermal-emission rates decrease with increasing reverse bias. Changes in peak temperature (and correspondingly in DLTS activation energies or emission rates) have been observed in detailed DLTS studies involving DX centers in AlGaAs of varying ternary composition.³¹ This activation energy dependence on electric field also had composition dependences. The tentative explanation given in that report was that multiple closely related peaks were observed, from slightly different defect configurations. If the concentration of a particular defect configuration is somehow field dependent, then different activation energies can be obtained from different bias conditions. Our observation of a broader DLTS peak from this defect(s) and its unusual change in peak shape with applied bias is consistent with this interpretation, and the peaks shown in Fig. 4 could very well originate from various slightly different interfacial defect configurations.

The increased intensity of the low temperature peak with shorter filling pulses in the n -InAlAs/AlGaAs structures can perhaps be understood from the larger cross sections measured for this peak. If we assume, that as we proposed, the low-temperature peak shown in Fig. 6 originates from interfacial defect levels in the InAlAs and AlGaAs barrier, DLTS experiments show that when the filling pulse is short, the multiple defect centers, or electron traps shown in Fig. 6, cannot be filled because they have a smaller capture cross section. The signal seen at lower temperatures, which we attribute to interfacial defects, is the only one seen for short filling pulses because carriers are not trapped by the center with the smallest capture cross section. The fact that this simple peak at low temperature can only be observed for

short filling pulses, and almost disappears at long filling pulses is unusual, and seems to indicate population of a defect center at the expense of the other center.

A couple of basic, general results can be concluded from these experiments. One of them is that defect centers in quantum dots have much different effects on QD optical properties depending on their atomic configuration, method of introduction, and most importantly, the spatial positioning of these defect centers with respect to QD localization. The defects caused by irradiation, as proton or electron induced displacement damage, would be expected to have different impact on optical properties, since the defects do form randomly and are distributed across the entire semiconductor chip, including the buffer layer and substrates. Most of these defects are therefore spatially far apart from the region of QD wave function confinement, and cannot serve as a recombination center for electrons and holes in the QD's. On the other hand, when defects are in close proximity to the dots, within the dots, or at the dot/barrier interface, their effects on optical emission are very significant, as is shown in this work. Another clear finding from these experiments is that even though DLTS can be sufficiently sensitive to detect electron and hole levels from QD states, it is in all practicality very difficult to detect them when defect concentrations near the dots (either at the dots or barriers) exceed the volumetric QD concentration, which as seen here can be easily achieved.

CONCLUSIONS

Red emitting multilayered InAlAs/AlGaAs quantum dots have been grown using MBE and inserted in pn diodes and Schottky barriers. We have shown that defects can have an important role in the optical and transport properties of multilayered QD structures in the InAlAs/AlGaAs material system, and can dominate the optical properties in these InAlAs/AlGaAs quantum dots; showing that further refinements in the growth process or in the passivation of interfacial defects should be performed before InAlAs/AlGaAs QD's could be used for efficient red light emitters. Photoluminescence lifetimes in these dots have been measured to be 6 and 29 ps in InAlAs QD's embedded in n and p AlGaAs diodes, respectively. Strong DLTS signals are found in both p - and n -type structures. In the p -type structure, a defect with an activation energy $E_a = 0.37$ eV in concentrations of $6 \times 10^{16} / \text{cm}^3$ was found. In the n -type samples, a complex peak structure was found for long filling pulses. Such peak structure is similar to what has been reported for DX -like centers in AlGaAs and InAlAs. A broader peak in the n -type samples was identified and isolated after reducing the filling pulse time. Such peak exhibits plateaus in the signal intensity when the applied bias is varied, and shows shifts in activation energy with increased applied bias. This peak has been identified as either a QD/barrier interfacial defect, or as originating from electron levels in InAlAs/ n -AlGaAs quantum dots. Further work reducing the defect density in these n -type samples is needed for an unambiguous identification of this peak.

ACKNOWLEDGMENTS

Part of this research was carried out at the Jet Propulsion Laboratory, California Institute of Technology, under a con-

tract with the National Aeronautics and Space Administration. Financial support from the Swedish Foundation for International Cooperation in Research and Higher Education (STINT) is gratefully acknowledged.

-
- ¹P. G. Piva, R. D. Goldberg, I. V. Mitchell, D. Labrie, R. Leon, S. Charbonneau, Z. R. Wasilewski, and S. Fafard, *Appl. Phys. Lett.* **77**, 624 (2000).
- ²R. Leon, G. M. Swift, B. Magness, W. A. Taylor, Y. S. Tang, K. L. Wang, P. Dowd, and Y. H. Zhang, *Appl. Phys. Lett.* **76**, 2074 (2000).
- ³S. Marcinkevicius, R. Leon, B. Čechavičius, J. Siegert, C. Lobo, B. Magness, and W. Taylor, *Physica B* **314**, 203 (2002).
- ⁴J. Zou, D. J. H. Cockayne, and B. F. Usher, *J. Appl. Phys.* **73**, 619 (1993).
- ⁵J. W. Matthews and A. E. Blakeslee, *J. Cryst. Growth* **27**, 118 (1974).
- ⁶S. Yu. Shiryayev, F. Jensen, J. L. Hansen, J. W. Petersen, and A. N. Larsen, *Phys. Rev. Lett.* **78**, 503 (1997).
- ⁷R. Leon, S. Chaparro, S. R. Johnson, C. Navarro, X. Jin, Y. H. Zhang, J. Siegert, S. Marcinkevicius, X. Z. Liao, and J. Zou, *J. Appl. Phys.* (to be published).
- ⁸J. M. Gerard, O. Cabrol, and B. Sermage, *Appl. Phys. Lett.* **68**, 3123 (1996).
- ⁹K. K. Linder, J. Phillips, O. Qasaimeh, X. F. Liu, S. Krishna, P. Bhattacharya, and J. C. Jiang, *Appl. Phys. Lett.* **74**, 1355 (1999).
- ¹⁰C. Lobo, Ph.D. dissertation, Australian National University, 2000.
- ¹¹H. Benisty, C. M. Sotomayor-Torres, and C. Weisbush, *Phys. Rev. B* **44**, 10 945 (1991).
- ¹²U. Bockelmann, *Phys. Rev. B* **48**, 17 637 (1993).
- ¹³S. Anand, N. Carlsson, M-E Pistol, L. Samuelson, and W. Seifert, *Appl. Phys. Lett.* **67**, 3016 (1995).
- ¹⁴H. L. Wang, F. H. Yang, S. L. Feng, H. J. Zhu, D. Ning, H. Wang, and X. D. Wang, *Phys. Rev. B* **61**, 5530 (2000).
- ¹⁵J. Ibañez, R. Leon, D. T. Vu, S. Chaparro, S. R. Johnson, C. Navarro, and Y. H. Zhang, *Appl. Phys. Lett.* **79**, 2013 (2001).
- ¹⁶R. Leon, P. M. Petroff, D. Leonard, and S. Fafard, *Science* **267**, 1966 (1995).
- ¹⁷R. Leon, S. Fafard, D. Leonard, J. L. Merz, and P. M. Petroff, *Appl. Phys. Lett.* **67**, 521 (1995).
- ¹⁸S. Marcinkevicius, J. Siegert, R. Leon, B. Čechavičius, B. Magness, W. Taylor, and C. Lobo (unpublished).
- ¹⁹S. Marcinkevicius, A. Gaarder, and R. Leon, *Phys. Rev. B* **64**, 115307 (2001).
- ²⁰S. Raymond, S. Fafard, S. Charbonneau, R. Leon, D. Leonard, P. M. Petroff, and J. L. Merz, *Phys. Rev. B* **52**, 17 238 (1995).
- ²¹D. V. Lang, *J. Appl. Phys.* **45**, 3023 (1974).
- ²²C. Hemmingsson, N. T. Son, O. Kordina, E. Janzen, and J. L. Lindström, *J. Appl. Phys.* **84**, 704 (1998).
- ²³J. Criado, A. Gomez, E. Calleja, and E. Munoz, *Appl. Phys. Lett.* **52**, 660 (1988).
- ²⁴M. M. Sobolev, I. V. Kochnev, V. M. Lantratov, N. A. Cherkashin, and V. V. Emtsev, *Physica B* **273-274**, 959 (1999).
- ²⁵Y. B. Jia, Z. Y. Han, H. G. Grimmeiss, and L. Dobaczewski, *J. Appl. Phys.* **80**, 2860 (1996).
- ²⁶K. J. Choi and J. L. Lee, *J. Vac. Sci. Technol. B* **19**, 615 (2001).
- ²⁷A. Malinin, H. Tomozawa, T. Hashizume, and H. Hasegawa, *Jpn. J. Appl. Phys.* **34**, 1138 (1995).
- ²⁸S. Dueñas, R. Pinacho, E. Castan, L. Quintanilla, R. Pelaez, and J. Barbolla, *J. Appl. Phys.* **82**, 4338 (1997).
- ²⁹P. Krispin, R. Hey, H. Kostial, and K. H. Ploog, *J. Appl. Phys.* **83**, 1496 (1998).
- ³⁰J. Frenkel, *Phys. Rev.* **54**, 647 (1938).
- ³¹Y. B. Jia and H. G. Grimmeiss, *Phys. Rev. B* **47**, 1858 (1993).